Midlatitude propagation of VLF to MF waves through nighttime ionosphere above powerful VLF transmitters

F. Lefeuvre, J. L. Pinçon, and M. Parrot

Received 9 November 2012; revised 7 February 2013; accepted 7 February 2013; published 12 March 2013.

[1] Midlatitude nighttime observations made by the DEMETER satellite in the very low frequency (VLF) to medium frequency (MF) bands (3 kHz to 3 MHz) have demonstrated the propagation of radio waves from the bottom of ionosphere up to the satellite altitude (~700 km). Propagation characteristics derived from the magneto-ionic theory [Budden, 1985] are used to explain the absence of wave observations between ~1 and 2 MHz. Under hypotheses made for the Appleton and Hartree (or Appleton and Lassen) formula, studies of the vertical variations of the real and imaginary parts of the refractive index are performed to point out modifications in the propagation characteristics of the waves: (i) at the crossing of the plasma cutoffs regions, (ii) at the crossing of the ordinary and extraordinary mode resonance regions, and (iii) in the region where the product of the collision frequency (v) and the electronic density (Ne) is maximum. It is shown that enhancements in the collision frequencies, produced by powerful VLF transmitters in the region where the product of v and Ne is maximum, open the half angle of the MF wave transmission cones and increase the power densities of those waves at the DEMETER altitude.

Citation: Lefeuvre F., J. L. Pinçon, and M. Parrot (2013), Midlatitude propagation of VLF to MF waves through nighttime ionosphere above powerful VLF transmitters, *J. Geophys. Res. Space Physics*, *118*, 1210–1219, doi:10.1002/jgra.50177.

1. Introduction

[2] Midlatitude nighttime observations made by the DEMETER satellite in the very low frequency (VLF) to medium frequency (MF) frequency bands (3 kHz to 3 MHz) have shown the propagation of radio waves from the bottom of the ionosphere up to the satellite altitude (~700 km) [*Parrot et al*., 2008, 2009; *Bell et al*. 2011]. The aim of the present paper is to review the propagation mechanism involved in transionospheric propagations and to point out those which can explain unexpected DEMETER observations.

[3] Unexpected DEMETER observations have been pointed out by *Parrot et al*. [2009] through statistical maps of midlatitude nighttime electric field observations [*Berthelier et al*., 2006] performed over a 3 year time period (2006–2008). A more complete set of maps is displayed in Figure 1.

[4] (i) The top panel (Figure 1a) provides the statistical map of observations made in the 18–25 kHz frequency band (the frequency band of most powerful transmitters). The numbers printed on the map indicate the location of those transmitters. The corresponding geographical parameters and transmitted powers are given in Table 1. High-power densities are observed over very wide geographical areas located at latitudes slightly below the ones of the transmitters and their conjugated regions, which is due to the fact that plasma waves propagate along the field lines. The effect is the most visible at the vicinity of the equatorial region. Case studies [*Parrot et al*., 2008] confirm the observation of well-defined signatures of VLF transmitters at the satellite altitude. They also point out the transionospheric penetration of lightning-generated wave energy whistlers. For the sake of convenience, those whistlers are called 0^+ whistler, i.e., zero-hop plus whistler that reaches the satellite over a short-direct upward path [*Smith and Angerami*, 1968; *Lefeuvre et al*., 2009].

[5] (ii) The bottom panel (Figure 1c) gives the statistical map of observations made in the 2–2.5 MHz frequency band. High-power densities are surprisingly observed over the same geographical areas than for VLF waves. Case studies over wider frequency bands [*Parrot et al*., 2008] show that the DEMETER observations made in the MF band are associated with intense 0^+ whistlers. They are characterized by a very sharp lower-frequency cutoff at ~1.75 MHz, a maximum around 2 MHz, then a decreasing slope up to ~2.5 MHz. The lightning origin of the observed MF waves has been successfully tested by *Parrot et al*. [2009].

[6] (iii) The mid panel (Figure 1b) gives the statistical map of observations made in the 1–1.6 MHz frequency band. A part for high latitudes, one does not observe any signature of 0^+ whistlers.

[1]Laboratoire de Physique et Chimie de l'Environnement et de l'Espace, CNRS, Orleans, France.

Corresponding author: F. Lefeuvre, LPC2E/CNRS, 3 A Av Recherche Scientifique, 45071 Orleans CEDEX 2, France. (francois.lefeuvre@cnrs-orleans.fr)

2169-9380/13/10.1002/jgra.50177

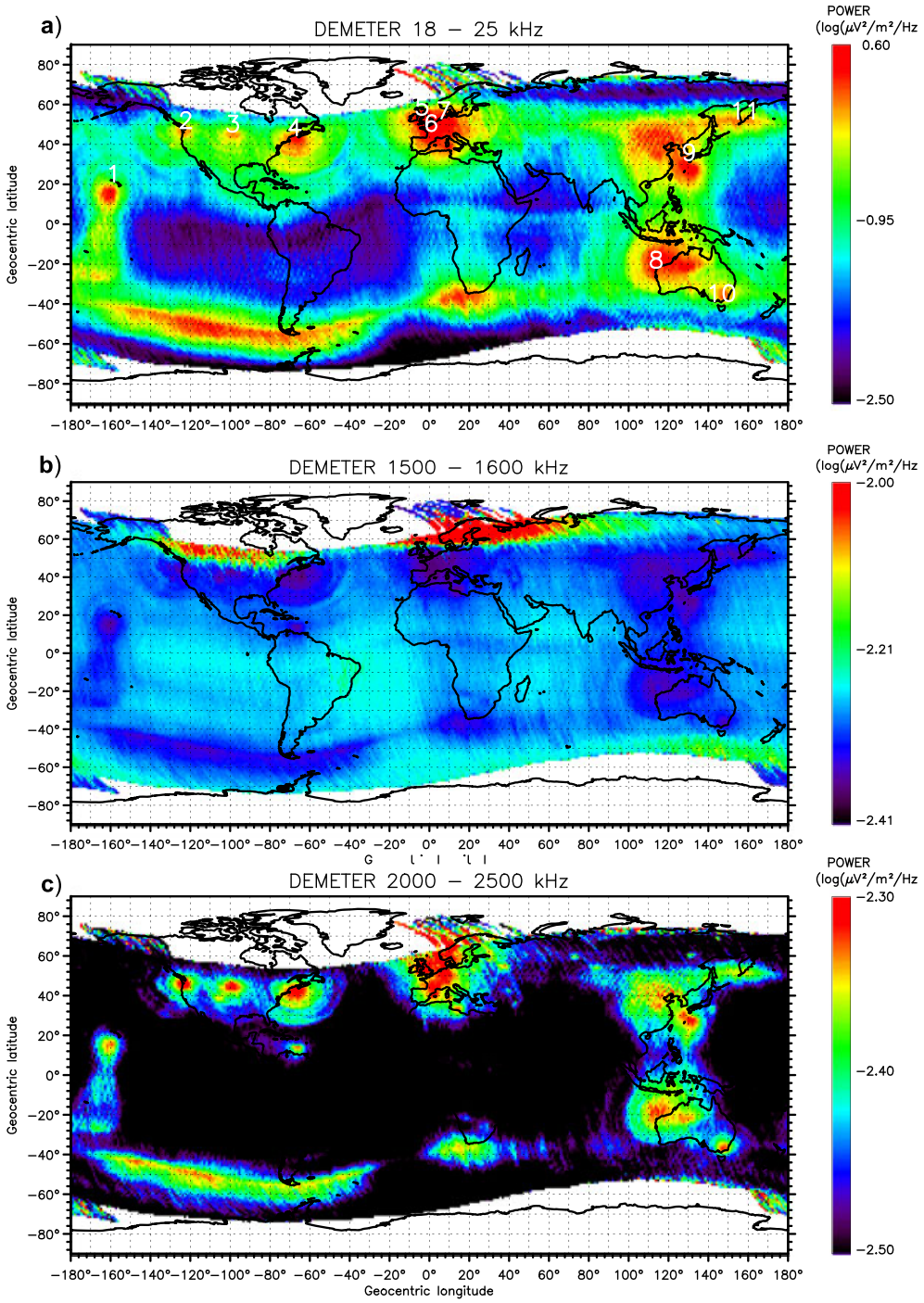

Figure 1. Statistical maps of DEMETER nighttime electric field observations performed over a 3 year time period [2006–2008] by *Parrot et al.* [2009] for three frequency bands: 18–25 kHz, (a) 2–2.5 MHz, (b) 1–1.6 MHz, and (c) 2–2.5 MHz.

[7] Those unexpected observations raise the following questions. How do the propagation mechanisms involved in transionospheric propagations may explain the absence of 0^+ whistlers' observations in the 1–1.6 MHz frequency band, and probably in a larger band? What could explain the level and the size of the geographical areas of the high-power densities observed in the 18–25 kHz frequency band, and probably in a larger band? What could explain the same type of observations in the 2–2.5 MHz frequency band? If answering the first question is relatively easy (conditions for transionospheric propagation of radio waves are given in textbooks like *Ratcliffe* [1959], *Helliwell* [1965], and *Budden* [1985]), answering the second and third questions looks much more delicate.

[8] The mechanism proposed here to explain the relatively high-power densities of VLF and MF waves above powerful VLF transmitters is based on the two following hypotheses.

Table 1. VLF Transmitters Seen in the Map of Figure 1a [*Hansen*, 1999][a]

	Code	Name	Location	Frequency (kHz)	Power (kW)
1	NPM	Lualualei	N21°25′ W158°09′	21.4	500
2	NLK	Jim Creek	N48°12′ W121°55′	24.8	200
3	NML	La Moure	N46°21′ W098°20′	25.2	250
4	NAA	Cutler	N44°38′ W067°16′	24.0	1000
5	GQD	Anthorn	N54°54′ W003°16′	19.6	45
6	HWU	Rosnay	N46°42′ E001°14′	18.3	400
7	DHO	Rhauderfehn	N53°04′ E007°36′	23.4	670
8	NWC	North West Cape	S21°48′ E114°09′	19.8	1000
9	NDT	Ebino	N32°04′ E130°49′	22.2	100
10	NTS	Woodside	S38°28′ E146°56′	18.6	
11	UBE	Petropavlovsk	N52°55′ E158°39′	16.2	

[a]When it is noted, the power is only indicative as most of these transmitters are used by the army (navy) of different countries. The U.S. and NATO sites send 200 bauds MSK.

[9] (i) Hypothesis 1—the transmission cone of radio waves propagating from the bottom of ionosphere to the DEMETER satellite altitude (~700 km) is controlled by local transmission cones taking place at the altitude(s) of mode conversion (~90 km altitude for VLF waves), where extraordinary mode waves are converted into ordinary mode waves.

[10] (ii) Hypothesis 2—they are two regions of VLF heating within the ionosphere: the first one pointed out by *Inan* [1990] in the D layer and, as suggested by *Bell et al*. [2011], promoted by *Kuo et al*. [2012], but refuted by *Moore et al*. [2012], and the second one located somewhere between the E layer and the ~700 km altitude. Enhancements in the collision frequencies induced by those heating sources open the local transmission cones.

[11] Following a technique already used in *Lefeuvre et al*. [2009], the study of that mechanism is conducted from the computation of the vertical variations of the real (μ) and negative imaginary (χ) parts of the refractive index ($n = \mu - i\chi$), the real part providing information on the propagation path, and the imaginary part on the absorption of wave energy. In order to stay in the framework fixed by *Budden* [1985] about the propagation of radio waves in the ionosphere, the computations of the refractive index is done by applying the Appleton-Hartree (or Appleton-Lassen) formula, where the electron collision frequency is assumed to be independent of the electron velocity. As noted by *Sen and Wyller* [1960], that hypothesis may be invalid when the collision frequency ν becomes nonnegligible compared to the angular frequency of the wave ω. This may be the case for the lower ionosphere and, whatever the altitude, for geographical longitudes where powerful VLF transmitters trigger electron precipitations [*Inan et al*., 1984; *Inan et al*., 1985; *Sauvaud et al*., 2008].

[12] For the sake of convenience, the ordinary and extraordinary modes will be noted "Ord" and "Ext" throughout the paper. They are the notations adopted by *Ratcliffe* [1959], *Helliwell* [1965], and *Budden* [1980] for studies of the propagation of radio waves through the ionosphere. They have the advantage to avoid any confusion between the X plasma parameter defined in the next section and the X notation often used for the extraordinary mode.

[13] The plan of the paper is as follows. In section 2, the main characteristics of the propagation paths followed by radio waves in the VLF to MF frequency range are reviewed. Section 3 is dedicated to the modeling of the propagation of VLF and MF waves through the ionosphere. The effects of heating on the propagation characteristics of those waves are examined in section 4. Section 5 concludes the paper.

2. Propagation Paths

[14] In radio communications, it is generally considered that a propagation path is the path through which EM waves travel from the physical location of an emission source to the receiver location. According to the wave frequencies and to the propagation medium, one generally observes that a part of the wave energy is lost. For interpreting observations made by the DEMETER satellite in the VLF to MF frequency range, one is interested both by the propagation paths through which waves generated below the ionosphere are transmitted up to the satellite altitude (~700 km) and by the propagation paths where wave energy is reflected and/or absorbed. As a wave generated below the ionosphere is composed of an ordinary (Ord) propagation mode and an extraordinary (Ext) propagation mode when it penetrates into the ionosphere [see, for instance, *Benson et al*., 1998], at each frequency there are at least two propagation paths: one for waves in the Ord mode at the bottom of ionosphere and the other for waves in the Ext mode. As it will be seen later on, according to the vertical variations of the refractive index, one may be led to split a propagation path into two or even three parts.

[15] Most propagation characteristics of radio waves may be derived from the Appleton-Hartree formula [*Budden*, 1985]. The refractive index n^2 is a function of $X = f_{pe}{}^2/f^2$ and $Y = f_{ce}/f$ parameters (with f the wave frequency, f_{pe} the electron plasma frequency, and f_{ce} the electron gyrofrequency), the θ angle made by the wave vector $\mathbf{k}$ with the Earth magnetic field $\mathbf{B}_0$, and a complex value noted $U = 1 - iZ$ in which $Z = \nu/\omega$, with ν the electron collision frequency and $\omega = 2\pi f$.

[16] It writes:

$$n^2 = 1 - \frac{(AX)}{B(X,Y,\theta) \pm C(X,Y,\theta)} \tag{1}$$

with

$$A(X) = X(U - X)$$
$$B(X,Y,\theta) = U(U - X) - \frac{Y_T^2}{2}$$
$$C(X,Y,\theta) = \left(\frac{Y_T^4}{4} + Y_L^2(U - X)^2\right)^{1/2}$$

and

$Y_T = Y \sin\theta$
$Y_L = Y \cos\theta$

[17] The + symbol in the denominator is attached to the Ord mode and the – symbol to the Ext mode.Dependence of n^2 on X for cold collisionless electron plasma ($\nu = 0$) has been extensively studied by *Budden* [1985]. The main results are the following.

[18] (i) One value of n^2, but only one, is zero when $X = 1 + Y$ or $X = 1 - Y$ or $X = 1$, the corresponding frequencies being called cutoff frequencies. For $X = 1 + Y$ or $X = 1 - Y$, the cutoff frequency applies to all θ values. For $X = 1$, the other nonzero value of n^2 is $n^2 = 1$. However, for the sake of convenience, we will continue to talk about the $X = 1$ cutoff.

[19] (ii) One value of n^2, but only one, is infinite when $X = X_\infty = (1 - Y^2)/(1 - Y^2\cos^2\theta)$. For $Y > 1$, resonances occur in the ordinary mode at $X > 1$, with two branches: one below X_∞, which is the one we will consider here, and the other one above, where $n^2 \to \infty$ when $X \to \infty$. For $Y < 1$, resonances occur in the Ext mode, the resonance for $\theta = \pi/2$ being the upper hybrid resonance.

[20] The X characteristic values defined here will be used to characterize propagation paths for waves in cold plasmas with collisions.

[21] Following *Ellis* [1956, 1962], *Budden* [1985] has developed what is generally called the radio-window concept. It is based on the existence of "window points," i.e., of points in space where the extraordinary and ordinary waves have the same value for their refractive index at the altitude of the $X = 1$ plasma cutoff. In a plasma where collisions are neglected, it is easily checked that such equalities are only possible for longitudinal waves ($\theta = 0°$ or π). There is only one "window point" from which a mode conversion is possible. In a plasma with collisions, the mode conversion becomes possible through a wider radio window. This radio window defines a propagation cone from which the converted radio wave appears to be transmitted. Analytical treatments are needed to compute the transparency of a radio window and the half angle of the transmitted cone. In the present paper, one will only look for the existing window points at different θ values and will derive the half angles of the transmission cones from those points.

[22] Let us first consider the $Y > 1$ waves (Table 2), i.e., in the present study, the VLF and LF frequencies plus the lowest frequency part of the MF waves. There are potentially two propagation paths (PP1 and PP2) starting at $X = 0$ (the bottom of the ionosphere): one from the Ext mode (PP1) and the other from the Ord mode (PP2). However, the PP1 propagation path must be divided in two parts: PP1-a for which the slope of $n^2(X)$ is >0 in the vicinity of $X = 1$, and PP1-b for which the slope of $n^2(X)$ is <0. Clearly, PP1-a is the only propagation path which may transfer energy from the bottom of the ionosphere ($X = 0$) up to the maximum of the F layer (X_{max}), then up to the satellite altitude (from X_{max} to lower X values). Wave energy may be lost: (i) at the crossings of the RW2 radio window (RW2 stands for "second radio window" [*Jones*, 1976; *Budden*, 1980]), where, after mode conversion, a part of the waves is transmitted, whereas the other part is reflected, and (ii) at the crossing of the O mode resonance region. Waves propagating along the PP1-b and PP2 propagation paths are stopped at the altitude where $X = 1 + Y$, i.e., at the altitude where $n^2 = 0$.

[23] It must be noted that Tables 2 and 3 may be read in both directions, i.e., from the ground to the magnetosphere (left to right) and from the magnetosphere to the ground (right to left).

[24] At frequencies such that $Y < 1$ (Table 3), a distinction must be made between propagation in a medium where the altitude of X_{max} is lower than that of $X = 1 + Y$ or smaller. In the first case ($X_{max} < 1 + Y$), there are potentially two propagation paths (PP3 and PP4) starting at the bottom of the ionosphere. The propagation path PP3 allows to transfer energy up to the maximum of the F layer and then to higher altitudes, whereas the PP4 propagation path is stopped at the altitude where $X = 1 - Y$. In the second case ($X_{max} > 1 + Y$), there are potentially two propagation paths (PP5-a and PP5-b) starting at the bottom of the ionosphere. However, both are stopped at the altitude where $X = 1 + Y$, i.e., at the altitude where $n^2 = 0$. Clearly, PP3 is the only propagation path which may transfer energy up to the satellite altitude. However, the wave energy

Table 2. $Y = f_{ce}/f > 1$, Propagation Paths From the Bottom of the Ionosphere to the Maximum of the F Layer[a]

	Y > 1			
X	**0**	**1**	**1+Y**	**X_{max}**
PP1-a	Ext mode ($n^2 \uparrow$)	**RW_2** / **Res**	Ord mode (whistler mode)	
PP1-b	Ext mode ($n^2 \downarrow$)			No propagation
PP2	Ord mode	**RW**	Ext mode	

[a]RW and RW2 are the *Budden's* [1985] radio windows. Propagation path PP1-a is the only one which allows to transfer energy up to the maximum of the F layer and then at higher altitudes. Res is the value of X where $n^2 \to \infty$. Waves propagating along PP1-b and PP2 are stopped at the altitude where $X = 1 + Y$, i.e., where $n^2 = 0$.

Table 3. $Y = f_{ce}/f < 1$, Propagation Paths From the Bottom of the Ionosphere to the Maximum of the F Layer[a]

	Y < 1				
X	**X_{max} < 1+Y**				
	0	**1-Y**	**1**	**X_{max}**	**1+Y**
PP3	Ord mode		**RW**	Ext mode	
PP4	Ext mode		No propagation		
X	**X_{max} > 1+Y**				
	0	**1-Y**	**1**	**1+Y**	**X_{max}**
PP5-a	Ord mode		**RW**	Ext mode ($n^2 \downarrow$)	No propagation
PP5-b	No propagation	**Res**	Ext mode ($n^2 \uparrow$)	←	

[a]RW and RW2 are *Budden's* [1985] radio windows. Propagation path PP3 is the only one which allows transferring energy up to the maximum of the F layer and then at higher altitudes. Waves propagating along PP4 or PP5-a are respectively stopped at the altitudes where $X = 1 - Y$ and $X = 1 + Y$, i.e., at the altitudes where $n^2 = 0$. Reflected waves propagating along PP5-b may reach the Ext mode resonance.

which is transferred depends on the transparency of the radio windows to be crossed at the entry into the ionosphere and then at the output.

[25] It is important to note that the condition $X_{max} < 1 + Y$ limits the frequency band of the $Y < 1$ waves which may reach the satellite altitude. As an example, taking f_{ce} = ~1.3 MHz and $(f_p)_{max}$ = 2.7 MHz, one observes that this condition can only be fulfilled for frequencies above ~2.15 MHz. In the frequency band 1.3–2.1 MHz, waves may propagate along propagation path PP5-a or PP5-b. However, they are stopped at the altitude where $X = 1 + Y$, i.e., at the altitude where $n^2 = 0$. This is what is observed on Figure 1b. For $X_{max} > 1 + Y$, 0^+ whistler cannot be observed at the DEMETER altitude.

3. Modeling

[26] In a plasma with collisions, i.e., when Z is not equal to zero, the values of n^2 given by equation (1) are complex. The propagation characteristics of the waves propagating from the bottom of ionosphere to the satellite altitude are derived, in the relevant propagation modes (PP1-a or PP3), from the vertical variations of the real (μ) and negative imaginary (χ) parts of the refractive index ($n = \mu - i\chi$) computed from a model of electron density profile and a model of collision profiles. Peaks in the χ values point out absorption regions, i.e., regions where wave energy is transmitted to the medium. They are heating regions.

[27] The electron density profile used in the present paper is displayed in Figure 2. It is derived from the 2007 IRI model [*Bilitza and Reinisch*, 2007], with date, time, and geophysical parameters (31 January 2006, 21:56 local time, latitude 32°, longitude 277°) from the DEMETER half-orbit 08687-1. The reasons for using these parameters are the following: (i) the corresponding density profile provides a good example of a "tenuous" nighttime density profile used by *Rodriguez* [1994] to estimate enhancements in the collision frequencies associated with VLF wave heating of ionosphere (31 January is one of the geomagnetic quietest day in 2006); (2) that density profile is located in a geographical region relatively far from powerful VLF transmitters, i.e., far from electron density changes due to heating by VLF transmitters [*Rodriguez and Inan*, 1994]; and (3) DEMETER observations performed along that orbit are well documented (see *Parrot et al.*, 2008, 2009).

[28] The collision frequency profile is more difficult to define. Below ~120 km (i.e., in the D and E layers), the collision frequency is generally supposed to be mainly due to electron-neutral collisions ν_{en}. In the absence of wave disturbance, the electron-neutral collision frequency can be written on the form [*Maslin*, 1976]:

$$\nu_{en}(h) = \nu_{en}(100)\exp\left[-0.17\,(h - 100)\right]\ \mathrm{sec}^{-1} \qquad (2)$$

with h the altitude in km and $\nu_{en}(100) = 5 \times 10^4$. That expression gives values very close to the *Wait and Spies* [1964] model derived from experimental data and used for nighttime conditions. At altitudes above ~120 km (i.e., in the F layer), the collision frequency is the sum of the electron-neutral ν_{en} and electron-ion collisions ν_{ei}.

[29] An attempt has been made by *Aggarwal et al.* [1979] to compute a unified model of the electron-collision frequency (here noted $\nu_A(h)$) from 50 to 500 km altitude. According to the authors, the main characteristics of that model are as

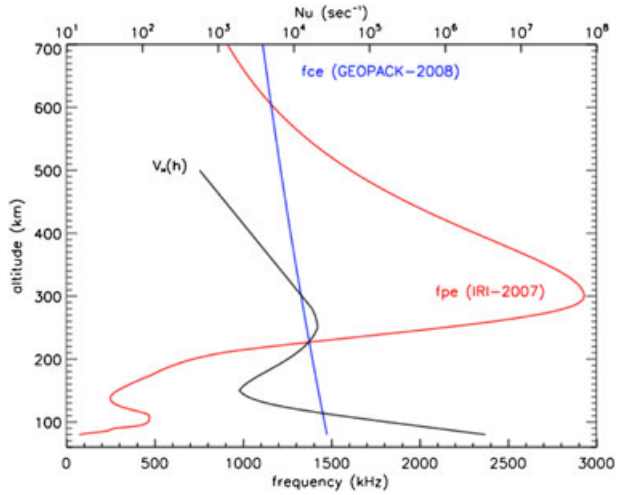

Figure 2. Electron density profile derived from the 2007 IRI model with date, time, and geophysical parameters of a DEMETER orbit (see section 4), and collision frequency profile ($v_H(h)$) derived from the *Aggarwa et al*. [1979] model and from experimental data.

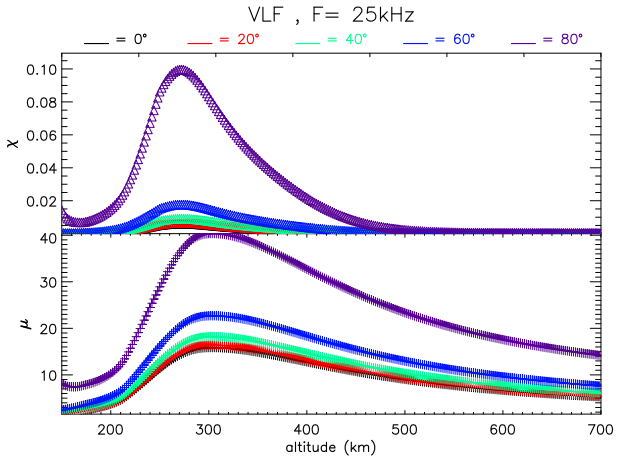

Figure 3. Second heating region. It is characterized by a maximum in the absorption level (χ values) of waves propagating at 25 kHz with θ values running from 0° to 80° (see color code). It corresponds to regions where the product of ν and Ne is maximum (see text).

follows: first, below ~150 km, an excellent agreement with the *Wait and Spies* [1964] and *Maslin* [1976] models, and second, above ~150 km, an underestimation of the experimental data by about a factor of 4. As an example, in the altitude range 120–400 km, the theoretical values vary from ~5×10^2 to 1.5×10^3 s^{-1} (the maximum value being at ~250 km altitude), and the experimental data from ~10^3 to 7×10^3 s^{-1}. More recent nighttime observations have confirmed this range of uncertainties [*Baulch and Butcher*, 1988; *Danilkin et al*., 2005]. As a consequence, the model which is used here is a hybrid model $v_H(h)$ such that $v_H(h) = v_A(h)$ for $h \leq 150$ km and $v_H(h) = 4\ v_A(h)$ for $h \geq 200$ km (see Figure 2).

[30] Simulations made for the lower ionosphere may be checked from results obtained by *Inan* [1990], *Inan et al*. [1992], *Rodriguez et al*. [1994], and *Rodriguez* [1994] by analyzing VLF signals generated by controlled experiments conducted from U.S. Navy VLF transmitters (in particular the NAA and NSS transmitters operated at 24.0 and 24.8 kHz, respectively). They pointed out the existence of a heating region with a peak at ~85 km altitude (D layer): this is the first heating region. *Rodriguez* [1994] showed that, for a tenuous density profile, VLF heating of the lower ionosphere could produce a relative enhancement in the local electron collision frequency of a factor ~2 at the peak altitude.

[31] Simulations made for higher altitudes are based on the *Maslin* [1976] remark that, when the collision frequency ν is negligible compared to the angular frequency of the wave ω, the maximum absorption occurs at altitudes where the product of the collision frequency ν and the electronic density Ne is maximum. One may consider that this altitude range corresponds to the second heating region looked for by *Bell et al*. [2011]. In the condition used for Figure 3, that second heating region peaks around 310 km altitude and extends from ~240 to 530 km altitude, i.e., between the E layer and the ~700 km altitude. Its efficiency depends, first, on the electron density profile (the heating increases with the maximum value of Ne) and, second, on the location of the maximum absorption which, for $Y < 1$ waves, may be different from the one of $(\nu N)_{max}$ (see section 4). This could explain disagreements between *Kuo et al*. [2012] and *Moore et al*. [2012] about the existence of a second heating region. Studies of the propagation characteristics of the waves generated by powerful VLF transmitters will show that the wave heating level is controlled by large θ waves.

4. Effects of VLF Heating on the Propagation Characteristics of VLF and MF Waves

[32] For the sake of convenience, vertical variations of the μ and χ values have been computed for $Y > 1$ waves propagating along propagation path PP1-a (see Table 2) and for $Y < 1$ waves propagating along propagation path PP3 (see Table 3). According to the electron density and collision frequency profiles of Figure 2,

[33] (i) $Y > 1$ waves have to cross (i) the lower altitude $X = 1$ plasma cutoff and its associated radio window RW2, (ii) the Ord mode resonance region, and (iii) the second heating region where the product of ν and Ne is maximum.

[34] (ii) $Y < 1$ waves have to cross the lower- and higher-altitude $X = 1$ plasma cutoff and their associated radio window RW, the two plasma cutoffs being located within the second heating region where the product of ν by Ne is maximum.

[35] In both cases, the computations are done: first, for a medium not previously heated by VLF transmitters ($\nu(h) = v_H(h)$); second, for a medium heated by powerful VLF transmitters ($\nu(h) = 2v_H(h)$ or more). Lightning-induced heating [*Inan et al*., 1993; *Inan et al*., 1992; *Farges et al*., 2007], for which reliable estimates of enhancements in collision frequencies are not available, will not be considered here. Instead, the effects of VLF powerful VLF transmitters on lightning-generated waves (0^+ whistlers) will be examined.

4.1. $Y > 1$ Waves

[36] The $Y > 1$ waves considered here are waves propagating at 25 kHz. Very similar results are obtained for all frequencies in the VLF frequency band. At higher frequencies, the interpretation is either made more difficult by successive

crossings of the $X = 1$ plasma cutoffs at the entry and the exit of the nighttime valley observed between the E and F layers ($f < 400$ kHz) or of less interest since longitudinal waves only may cross the $X = 1$ plasma cutoffs ($f \geq 400$ kHz).

4.2. Propagation in a Medium Not Previously Heated ($\nu(h) = \nu_H(h)$)

[37] Let us first consider the crossing of the low-altitude $X = 1$ plasma cutoff which is indicated by the vertical dotted line in Figure 4a. It occurs at ~81.5 km altitude. The waves propagate in the Ext mode below 81.5 km and then in the Ord mode above. The only Ext mode waves which are converted into Ord mode waves are those for which a continuity is observed in the μ and χ values at $X = 1$ (window points). As shown in Figure 4a, this condition is fulfilled only for waves associated with θ values $\leq 20°$. Although limited space resolution (100 m) of the figure prevents to clearly identify it, the μ values of waves with θ values $\geq 30°$ tend to zero when $X \rightarrow 1$. This means that the waves which do not cross the radio window are reflected back. The presence of waves with θ values $\geq 30°$ above $X = 1$ only means that Ord mode waves may be generated there or may have been propagated from higher altitudes. As a consequence, one may consider that the half angle of the transmission cone at the output of radio window RW2 is on the order of 20°.

[38] The crossing of the Ord mode conversion region is illustrated by Figure 5a. Being located just above the RW2 radio window (see propagation path PP1-a, Table 2), it is only crossed by waves with θ values $\leq 20°$. The peak in χ values for waves associated with $\theta = 20°$ characterizes a wave absorption (or wave heating of ionosphere) region located at ~85 km altitude. This is precisely the altitude of the first heating region derived from the controlled experiments conducted from the VLF NAA and NSS transmitters [*Inan*, 1990]. Its lower and upper limits can be roughly estimated by considering the altitudes associated with half the maximum of the χ value for waves with

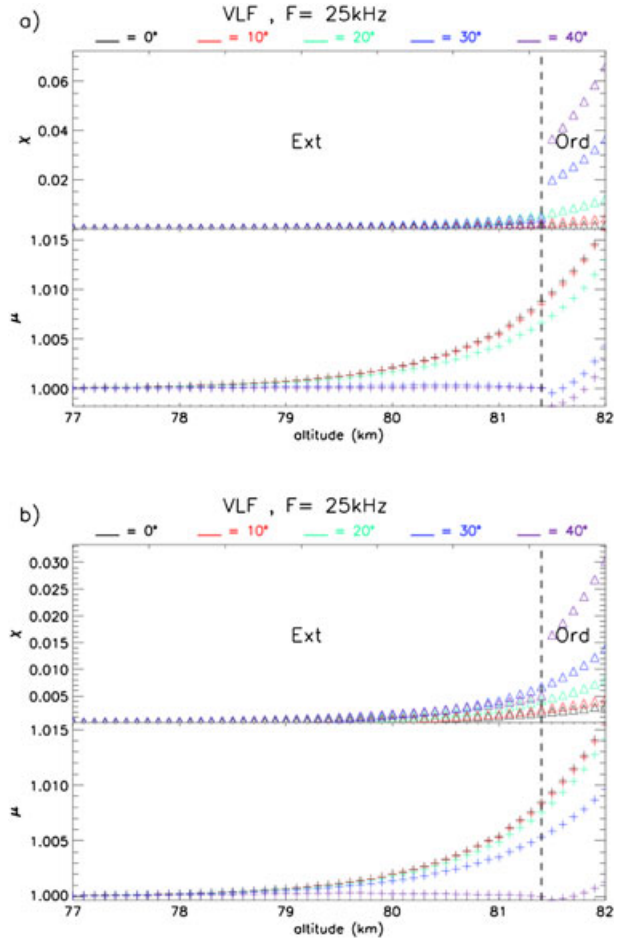

Figure 4. Crossing of the low-altitude $X = 1$ plasma cutoff (the vertical dotted line) by waves propagating at 25 kHz. The waves propagate with θ values running from 0° to 40° (see color code). They are in the Ext mode below the altitude of $X = 1$ and in the Ord mode above. Continuities in the μ and χ values at $X = 1$ mean that Ext mode waves have been converted into Ord mode waves which propagate to higher altitudes. The half angle of the transmission cone is equal to (a) ~20° for $\nu(h) = \nu_H(h)$ and (b) ~30° for $\nu(h) = 2\ \nu_H(h)$. Discontinuities in the μ and χ values mean that the waves observed below and above $X = 1$ are disconnected (see text).

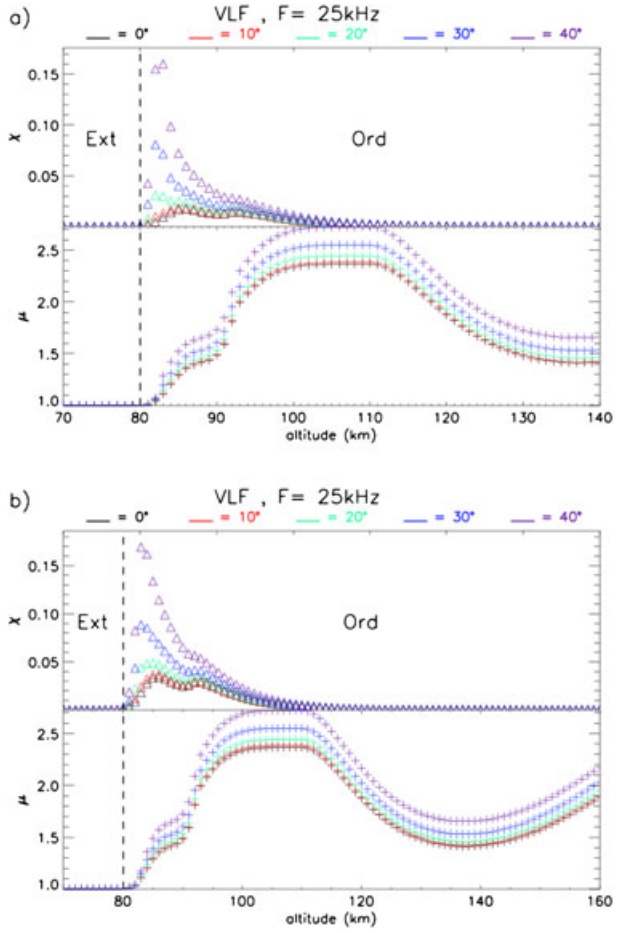

Figure 5. Crossing of the Ord mode resonance region by waves propagating at 25 kHz. The Ord mode resonance region is characterized by a "bump" in the μ values and peaks in χ values extending from ~82 to 95 km altitude. The absorption (or heating) levels may be estimated from the surfaces respectively created by the (a) $\theta = 20°$ curve for $\nu(h) = \nu_H(h)$ and (b) $\theta = 30°$ curve for $\nu(h) = 2\ \nu_H(h)$.

$\theta = 20°$. They cover the 82–95 km altitude range. The first heating region is in fact the Ord mode resonance region. A computation of the amount of heat produced by the VLF transmitter at 25 kHz and so of the induced enhancement in the collision frequency would require taking into account the total received power inside this region. Following *Rodriguez* [1994], one can make the assumption that the VLF heating of the lower ionosphere induces enhancements in the collision frequencies by a factor 2.

[39] As already mentioned, the second heating region, or region where the product of the collision frequency ν and the electronic density Ne is maximum, may be characterized from the peak in χ values observed in Figure 3. Its maximum value provides an estimation of the expected heating level. It is lower than in the first heating region for θ values lower than ~60° and higher above. Its width at half the maximum value indicates the altitude range of the heating region. Whatever the θ values, it extends from ~230 to ~340 km altitude.

[40] Observations of density depletions made by *Bell et al.* [2011] above the NWC and NAA VLF transmitters suggest that strong wave heating of the ionosphere may be observed above powerful VLF transmitters in that second heating region. Indeed, as shown by *Strelstov et al.* [2012], waves which propagate in those density depletions are close to the Gendrin mode defined by the condition $\cos\theta = 2f/f_H$ [*Gendrin*, 1961], i.e., in the condition displayed in Figure 2, may reach θ values up to ~87°, with, as a consequence, peaks in χ values much larger and much wider than in the first heating region. However, the absence of statistical information on the occurrence of the density depletions prevents to evaluate the effect of that strong wave heating on the medium and in particular on the enhancements in collision frequencies. A supplementary point to be examined in the future is the contribution of manmade and natural waves of higher frequencies in the heating region of the ionosphere between ~240 and ~340 km altitude. That point will be briefly discussed in the part devoted to $Y < 1$ waves.

4.3. Propagation in a Medium Previously Heated ($\nu(h) = 2\nu_H(h)$)

[41] Increasing the collision frequencies by a factor of ~2, one observes,

[42] (i) at the crossing of the RW2 radio window (Figure 4b), a slight increase in the altitude of the vertical $X = 1$ line and a significant increase in the value of the half angle of the transmission cone (here from ~20° to ~30°), and

[43] (ii) at the crossing of the Ord mode resonance (Figure 5b), an enhancement by a factor of ~3 in the absorption (or heating level).

4.4. $Y < 1$ Waves

[44] The effects of VLF heating on the propagation of MF wave concern here waves with frequencies extending from ~2.2 to 2.8 MHz. They are the only ones which propagate along propagation path PP3 (see Table 3) and cross the ionosphere. They do not cross any resonance region. The waves with frequencies below 2.1 MHz are reflected back at altitudes where $1 \le X < 1 + Y$ (propagation paths PP5), and the waves with frequencies above 2.8 MHz propagate in free space. The reflected waves either are converted into the Ord mode (propagation path PP5-a) or have access to the Ext mode resonance (propagation path PP5-b) with a possible contribution to the heating of ionosphere in the 200–250 km altitude range.

[45] Simulations have been performed at 2.2 MHz to point out the behaviour of MF waves at the crossing of the low altitude plasma cutoff and at the crossing of the high altitude plasma cutoff. A first simulation was performed for $\nu(h) = \nu_H(h)$, and a second for $\nu(h) = 3\ \nu_H(h)$. Considering the density profile given in Figure 2, the crossings of the low- and high-altitude plasma cutoff occur at ~259 and ~390 km altitudes, respectively. The corresponding results are displayed in Figures 6 and 7. The results are very similar whatever the frequency in the 2.2–2.8 MHz frequency band.

[46] At the crossing of the low altitude $X = 1$ cutoff, continuities in θ curves point out transmission cones with a half angle of 1° for $\nu(h) = \nu_H(h)$ (Figure 6a) and of 4° for $\nu(h) = 3\nu_H(h)$ (Figure 6b). At the crossing of the high altitude $X = 1$ cutoff, the half angle of the transmission cone increases from 1° for $\nu(h) = \nu_H(h)$ (Figure 7a) to $\nu(h) = 3\nu_H(h)$ (Figure 7b).

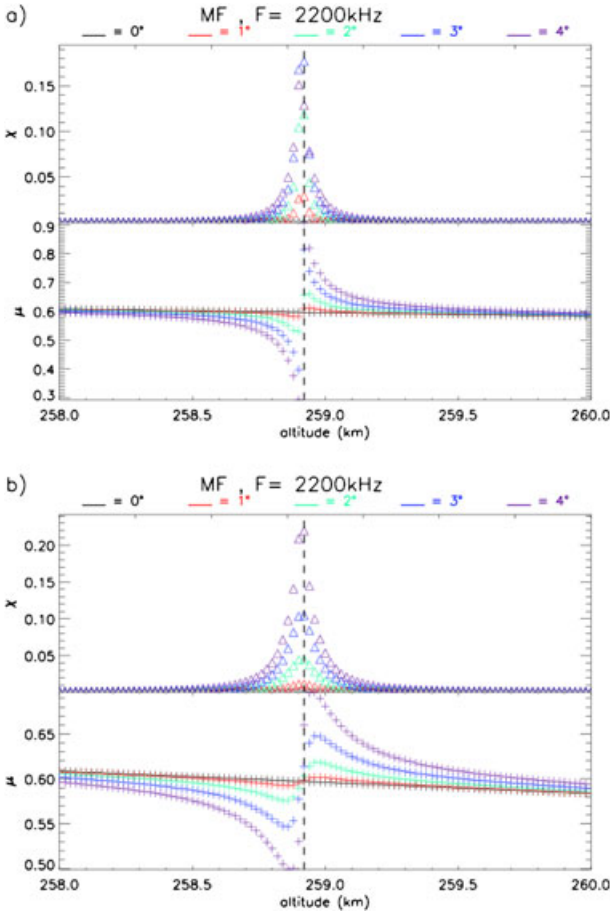

Figure 6. Crossing of the low-altitude $X = 1$ cutoff (the vertical dotted line) by waves propagating at 2.2 MHz. They propagate in the Ord mode below the altitude of $X = 1$ and in the Ext mode above. Continuities in the μ and χ values at the altitude of the vertical dotted lines mean that Ord mode waves have been converted into Ext mode waves which may propagate to higher altitudes. The half angle of the transmission cone opens from (a) 1° for $\nu(h) = \nu_H(h)$ to (b) 4° for $\nu(h) = 3\ \nu_H(h)$.

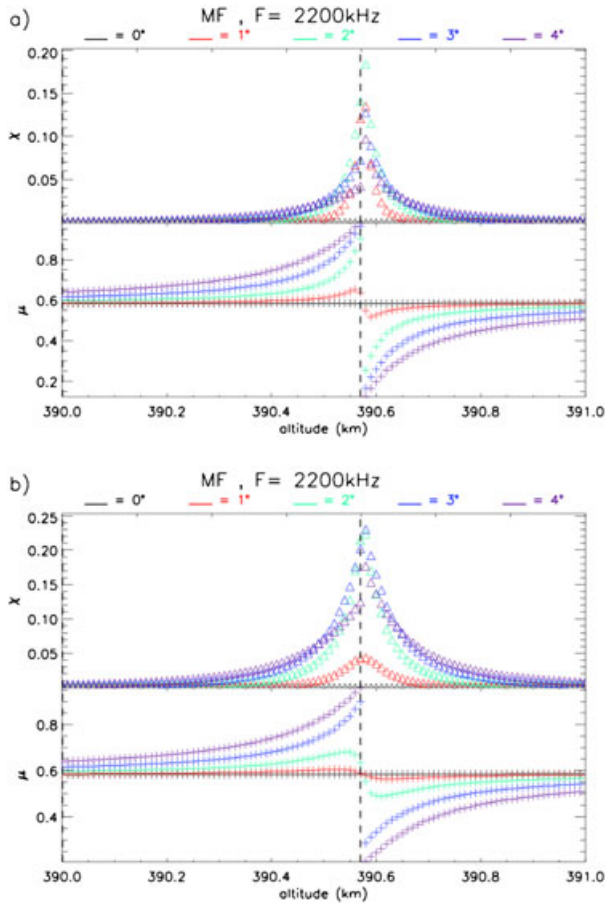

Figure 7. Crossing of the high-altitude $X = 1$ cutoff (the vertical dotted line) by waves propagating at 2.2 MHz. They propagate in the Ext mode below the altitude of $X = 1$ and in the Ord mode above. Continuities in the μ and χ values at the altitude of the vertical dotted lines mean that Ext mode waves have been converted into Ord mode waves which may propagate to higher altitudes. The half angle of the transmission cone opens from (a) 1° for $v(h) = v_H(h)$ to (b) 2° for $v(h) = 3\ v_H(h)$.

Although the opening of the transmission cone may be considered as relatively weak in both cases, they validate the hypothesis that enhancements in the collision frequencies (induced by VLF powerful transmitters) have an effect on the opening of the transmission cones of MF waves propagating from the bottom of the ionosphere up to the satellite altitude. The waves which are not transmitted being reflected back, vertical variations of the χ values point out peaks centered on the low- and high-altitude plasma cutoffs. In the conditions of Figures 6 and 7, those peaks are larger than the peak at $(v.\mathrm{Ne})_{maxv}$.

[47] Simulations performed with higher values of the electron density profiles would have for effects, first, to open the transmission cones, i.e., to transfer more wave energy, and, second, to reduce the peak in χ values around the low- and high-altitude plasma cutoffs. However, a full set of simulations with different density profiles is needed to fully understand Figures 1a and 1c and, in the same time, to fully characterize the second heating region. Complementary studies are also needed for evaluating the impact of analyses from *Sen and Wyller* [1960] which takes into account the electron velocity in the Appleton-Hartree formula.

5. Conclusion

[48] The present paper has been constructed around two questions raised by midlatitude nighttime observations made by the DEMETER satellite: first, the presence of 0^+ whistler emissions below ~1 MHz and above ~2 MHz, but not in between, and second, the high-power densities of VLF and MF waves observed over geographical areas located above VLF powerful transmitters.

[49] As shown in section 2, the answer to the first question is straightforward. At frequencies below the local electron gyrofrequency ($Y = f_{ce}/f > 1$), all waves generated below the ionosphere may cross the low-altitude cutoff (plus the high-altitude plasma cutoff for frequencies above ~1 MHz) and propagate up to the DEMETER altitude. At frequencies above the local electron gyrofrequency ($Y < 1$), the propagation through the ionosphere depends on the $X_{max} = f_{pe}^2/f^2$ value at the maximum of the F region. Waves with frequencies such as $X_{max} > 1 + Y$ are absorbed or reflected back at altitudes where $1 < X < 1 + Y$, whereas waves propagating with frequencies such as $X_{max} < 1 + Y$ may cross the ionosphere.

[50] The answering to the second question was much more delicate. However, the hypotheses made in the paper—(i) that they are two regions of VLF heating in the ionosphere, and (ii) that enhancements in the collision frequencies induced by those heating regions open the transmission cone of VLF and MF wave propagating through the ionosphere—have been validated. The technique used for those validations was the study of the vertical variations of the real (μ) and negative imaginary (χ) parts of the refractive index n ($n = \mu - i\chi$) computed from the Appleton-Hartree formulas, the real part providing information on the propagation path and the imaginary part on the absorption of wave energy, or which is the same on the wave heating of ionosphere. The main results are given below.

[51] Two heating regions are generated by powerful VLF transmitters: one in the D layer and the other in the F layer. The first one was pointed out and then characterized by analyzing VLF signals generated by controlled experiment conducted from U.S. Navy VLF transmitters [*Inan*, 1990; *Inan et al*., 1992; *Rodriguez et al*., 1994; *Rodriguez*, 1994]. The second one, postulated by *Bell et al*. [2011], was pointed out and characterized in the present paper. The new results are the following.

[52] (i) The D layer heating region is in fact the Ord mode resonance region (see propagation path PP1-a, Table 2), the heating level being a function of the wave normal directions in that region.

[53] (ii) The second heating region is located in the F layer, at altitudes where the product of Ne and v is a maximum [*Maslin*, 1976]. Its efficiency depends, first, on the electron density and collision frequency profiles and, second, on the location of the maximum absorption which, for frequencies greater than the local electron gyrofrequency ($Y < 1$), may be different from the one of $(vN)_{max}$. This could explain disagreements between *Kuo et al*. [2012] and *Moore et al*. [2012] about the existence or not of a second heating region. Observations of density depletions made by *Bell et al*. [2011] above the NWC and NAA VLF

transmitters suggest that strong wave heating of the ionosphere may be observed above powerful VLF transmitters in that heating region. However, the absence of statistical information on the occurrence of the density depletions prevents from evaluating the effect of that strong wave heating on the medium and in particular on the enhancements in collision frequencies.

[54] The transmission cones of radio waves propagating from the bottom of ionosphere to the DEMETER altitude (~700 km) are controlled by the transmission cones at the output of the radio windows located at the altitude of the $X = 1$ plasma cutoffs. Estimations of the half angles of those transmission cones are derived from a tenuous electron density profile.

[55] (i) At frequencies below f_{ce} ($Y > 1$), the waves reach the satellite after having crossed the low-altitude $X = 1$ plasma cutoff only. At 25 kHz, enhancements in the collision frequencies induced by the first heating region open the half angle of the transmission cone up to ~30°.

[56] (ii) At frequencies above f_{ce} ($Y < 1$), the waves cross the low-altitude and then the high-latitude $X = 1$ plasma cutoffs. At 2.2 MHz, enhancements in the collision frequencies induced by the second heating regions open the half angles of the low- and high-altitude $X = 1$ plasma cutoffs of a few degrees only. Higher electron density profiles are expected to transmit larger cones.

[57] A full interpretation of the high-power densities measured in the VLF and MF frequency ranges above powerful VLF transmitters [*Parrot et al*., 2008, 2009; *Sauvaud et al*., 2008] as well as of the extension of the geographical areas where they are observed would require a more accurate estimation of enhancements in the collision frequencies inside the second heating region and/or the introduction of the electron velocity in the Appleton-Hartree formula [*Sen and Wyller*, 1960].

[58] **Acknowledgments.** This work was supported by the Centre National d'Etudes Spatiales (CNES). It is based on observations with the electric field experiment ICE embarked on DEMETER. The authors thank J. J. Berthelier, the PI of the electric field experiment, for the use of the data and P. Hansen for information on the VLF station radiated power. They are very grateful to both reviewers for very helpful comments and suggestions.

References

Aggarwal K. M., N. Nath, and C. S. G. K. Setty (1979), Collision frequency and transport properties of electrons in the ionosphere, *Planet. Space Sci.*, *27*, 753–768.

Baulch, R. N. E., and E. C. Butcher (1988), Effective electron collision frequency measurements in the E-F regions, *J. Atmos. Terr. Phys.*, *50*(1), 45–49.

Bell, T., K. Graf, U. S. Inan, D. Piddyachiy, and M. Parrot (2011), DEMETER observations of ionospheric heating by powerful VLF transmitters, *Geophys. Res. Lett.*, *38*, L11103, doi:10.1029/2011GL047503.

Benson, R. F., B. W. Reinisch, J. L. Bougeret, R. Manning, D. L. Carpenter, D. L. Gallagher, P. H. Reiff, and W. W. L. Taylor (1998), Magnetospheric Radio sounding on the IMAGE mission, *Radio Sci. Bull.*, *285*, 9–20.

Berthelier, J. J., et al. (2006), ICE, the electric field experiment on DEMETER, *Planet. Space Sci.*, *54*, 456–471, doi:10.1016/jpss.2005.10.016.

Bilitza, D., and Reinisch, B. (2007), International Reference Ionosphere 2007: Improvements and new parameters, *J. Adv. Space Res.*, *42*(4), 599–609, doi:10.1016/j.asr.2007.07.04.

Budden, K. G. (1980), The theory of radio windows in the ionosphere and magnetosphere, *J. Atmos. Terr. Phys.*, *42*, 287–98.

Budden, K. G. (1985), The propagation of radio waves, Cambridge University Press.

Danilkin, N. P., P. F. Denisenko, B. G. Barabashov, and G. G. Vertogradov (2005), Electron collision frequency and HF waves attenuation in the ionosphere, *Int. J. Geomagn. Aeron.*, *5*, GI3009, doi:10.1029/2004GI000081.

Ellis, G. R. (1956), The Z propagation hole in the ionosphere, *J. Atmos. Terr. Phys.*, *8*, 243.

Ellis, G. R. (1962), Use of Z-mode propagation for observing cosmic radio noise from earth satellite, *Nature*, *193*, 862.

Farges, T., E. Blanc, and M. Tanguy (2007), Experimental evidence of D region heating by lightning-induced electromagnetic pulses on MF radio links, *J. Geophys. Res.*, *112*, A10302, doi:10.1029/2007JA012285.

Gendrin, R. (1962), Le guidage des whistlers par le champ magnétique, *Planet. Space Sci.*, *5*(4), 274.

Hansen, P. (1999), High power very low frequency/low frequency transmitting antennas, IEEE MILCOM, Monterey, CA.

Helliwell, R. A. (1965), Whistlers and related ionospheric phenomena, Stanford Univ. Press, Stanford, Calif.

Inan, U. S., H. C. Chang, and R. A. Helliwell (1984), Electron precipitation zones around major ground-based VLF signal sources, *J. Geophys. Res.*, *89*, 2981–2906.

Inan, U. S., H. C. Chang, R. A. Helliwell, W. L. Imhof, J. B. Reagan, and M. Walt (1985), Precipitation of radiation belt electrons by man-made waves: A comparison between theory and measurements, *J. Geophys. Res.*, *90*, 359–369.

Inan, U. S. (1990), VLF heating of the lower ionosphere, *Geophys. Res. Lett.*, *17*(6), 729–732.

Inan, U. S., J. V. Rodriguez, S. Lev-Tov, and J. Oh (1992), Ionospheric modification via a VLF transmitter, *Geophys. Res. Lett.*, *19*, 2071–2074.

Inan, U. S., J. V. Rodriguez, and V. P. Idone (1993), VLF signatures of lightning-induced heating and ionization of the nighttime D region, *Geophys. Res. Lett.*, *20*(21), 2355–2358.

Jones, D. (1976), The second Z-propagation radio, *Nature*, *262*, 674.

Kuo, S., A. Snyder, P. Kossey, C.-L. Chang, and J. Labenski (2012), Beating HF waves to generate VLF waves in the ionosphere, *J. Geophys. Res.*, *117*, A03318, doi:10.1029/2011JA017076.

Lefeuvre, F., R. Marshall, J. L. Pinçon, U. S. Inan, D. Lagoutte, M. Parrot, and J. J. Berthelier (2009), On remote sensing of transient luminous event's parent lightning discharges by ELF/VLF wave measurements on board a satellite, *J. Geophys. Res.*, *114*, A09303, doi:10.1029/2009JA014154.

Maslin, N. M. (1976), Estimating ionospheric cross-modulation, *Proc. R. Soc. London A*, *351*, 277–293.

Moore, R. C., S. Fujimaru, M. Cohen, M. Golkowski, and M. J. McCarrick (2012), On the altitude of the ELF/VLF source region generated during "beat-wave" HF heating experiments, *Geophys. Res. Lett.*, *39*, L18101, doi:10.1029/2012GL053210.

Parrot, M., U. Inan, N. Lehtinen, E. Blanc, and J. L. Pinçon (2008), HF signatures of powerful lightning recorded on DEMETER, *J. Geophys. Res.*, *113*, A11321, doi:10.1029/2008JA013323.

Parrot, M., U. S. Inan, N. G. Lethinen, and J. L. Pinçon (2009), Penetration of lightning MF signals to the upper ionosphere over VLF ground-based transmitters, *J. Geophys. Res.*, (2009), 114, A12318, doi:10.1029/2009JA014598.

Ratcliffe, J. A. (1959), The Magneto-Ionic Theory and Its Applications to the Ionosphere, Cambridge Univ. Press, Cambridge, U. K.

Rodriguez, J. V. (1994), Modification of the Earth's ionosphere by very-low-frequency transmitters, PhD thesis, Stanford University.

Rodriguez, J. V., and U. S. Inan (1994), Electron density changes in the nighttime D region due to heating by very-low-frequency transmitters, *Geophys. Res. Lett.*, *21*(2), 93–96.

Rodriguez, J. V., U. S. Inan, and T. F. Bell (1994), Heating of the nighttime D region by very low frequency transmitters, *J. Geophys. Res.*, *99*(A12), 23,329–23,338.

Sauvaud, J. A., R. Maggiolo, C. Jacquey, M. Parrot, J. J. Berthelier, R. J. Gamble, and C. G. Rodger (2008), Radiation belt electron precipitation due to VLF transmitters: Satellite observations, *Geophys. Res. Lett.*, *35*, L09101, doi:10.1029/2008GL033194.

Sen, H. K., and A. A. Wyller (1960), On the generalization of the Appleton-Hartree magnetoionic formulas, *J. Geophys. Res.*, *65*, 3391–3950.

Smith, R. L., and J. J. Angerami (1968), Magnetospheric properties deduce from OGO 1 observations of ducted and nonducted whistlers, *J. Geophys. Res.*, *73*, 1–20, doi:10.1029/JA073i001p00001.

Strelstov, A. V., J. R. Woodroffe, and J. D. Huba (2012), Propagation of whistler mode waves through the ionosphere, *J. Geophys. Res.*, *117*, A08302, doi:10.1029/2012JA017886.

Wait, J. R., and K. P. Spies (1964), Characteristics of the Earth-ionosphere waveguide for VLF radio waves, NSB Tech. Note U.S., 300.